Detection of movement of hemozoin crystals in the digestive vacuole of malaria parasites

Vanessa Alexandra Magalhães Costa
Under supervision of Professor Patrícia Maria Cristovam Cipriano Almeida de Carvalho
IST, Lisbon, Portugal
December, 2014

Abstract
Malaria results from protozoan infection of red blood cells by four species of *Plasmodium*, of which *falciparum* is the worst. In the intra-erythocytic cycle the parasite evolves through three stages: ring, trophozoite and schizont. The digestion of hemoglobin releases high quantities of toxic heme, which the parasite crystallizes into hemozoin in the digestive vacuole. This crystallization is a dynamic process, which is poorly understood. The analysis of the crystals' movement is the focus of this work. The hemozoin movement in the digestive vacuole of parasites in trophozoite stage was studied at room temperature after culturing at 37°C and after exposure to 40°C and 41°C for 1 hour through real-time microscopy using a high-speed camera coupled to an optical microscope. MegaSpeed and FastCam cameras were used to acquire image sequences at 2128, 4000, 7500 and 15000 fps. The frames were analyzed using scripts developed in ImageJ and Matlab. The average projected displacement of the particles is 0.236±0.090 μm (2128 fps) and 0.190±0.083 μm (4000 fps) and the average velocity is 52.5±21.3 μm/s (2128 fps) and 64.7±25.2 μm/s (4000 fps). The exposure to febrile temperatures dampened the hemozoin movement. However, the hemozoin movement partially resumed after 1 hour at room temperature for the heat treatment at 40°C. This demonstrates that the phenomenon is not Brownian. The apparently high driving force involved in this activity suggests that the phenomenon plays a vital role and that forced immobilization may lead to parasite destruction and innovative therapies.

Keywords: Malaria, hemozoin, movement, velocity, temperature, digestive vacuole

Introduction

Malaria is known as one of the most common and lethal parasitic infections in the world. About 40% of the world's population lives in malaria-endemic areas and this disease is responsible for up to 500 million episodes of clinical infection and 2.7 million deaths every year. It is estimated that in 2012 malaria caused 627 000 deaths mostly among African children [1, 12].

Malaria is found all over the tropical and subtropical regions of the world. The intensity and the pattern of transmission of malaria may differ noticeably within the same country as a result of variations in altitude or rainfall, social and environmental factors, coverage of health services and malaria control activities [2].

Malaria results from a protozoan infection of red blood cells caused in humans by four species of the genus *Plasmodium*, of which *falciparum* is the worst, while the other species that induce malaria are rarely deathly or responsible for persistent squeals. The transmission results exclusively through the bite of an infected female anopheline mosquito [1, 2].

Malaria typically presents symptoms of a nonspecific flu-like illness, with fever (every 48–72 hours), chills, headache, muscle aches, nausea, anorexia, and fatigue. The severity and course of an attack is related to the species and strain of the infecting parasite, as well as the age, genetic constitution, malaria-specific immunity, general health, and nutritional status of the patient, and on previous antimalarial drug use. The clinical condition of a nonimmune person with *falciparum* malaria who is untreated or in whom effective antimalarial treatment is delayed will

deteriorate quickly, probably resulting in severe disease and death [2].

To discuss the challenges connected to malaria therapy, the complexity of the disease should be taken into consideration and the biological aspects of the parasite at different stages of its development in infected humans must be understood. The life cycle of malaria (see figures 2 and 3) in a human host begins when the infected mosquito bites the person. The inoculated sporozoites migrate to the liver and invade the hepatocytes by mechanisms not entirely understood. Each sporozoite generates thousands of new parasites that are released into the bloodstream as merozoites, an invasive form fit to start the asexual blood stages in red blood cells (RBC), known as the intra-erythrocytic cycle. After invasion the parasite stays relatively inactive metabolically for 10–15 hours (the ring stage); then begins to ingest and digest hemoglobin (Hb) as it matures to trophozoite (a phase of rapid growth over the next 25 hours). In the final schizont stage the parasite digests the greater part of the hemoglobin and grows to fill more than 50% of the volume of the host cells, dividing into thousands merozoites that 48 hours after invasion lyse the RBC to be released into the bloodstream, restarting a new cycle. In most of the intra-erythrocytic cycle the parasite remains relatively hidden in the host cells and malaria is asymptomatic. However, exposure to the host immune system at the invasion stage turns the released merozoites into the principal etiological agents of malaria, causing the classical symptoms of the disease to manifest around two weeks after the mosquito-vectored sporozoite inoculation. During the intra-erythrocytic cycle the *P. falciparum* parasite consumes up to 80% of the host cell hemoglobin [27]. The digestion of hemoglobin releases high quantities of heme (a toxic compound lethal to the parasite) which the parasite crystallizes into paramagnetic hemozoin crystals (malaria pigment) (HZ) in its digestive vacuole (DV) [28]. Polymerization of heme into HZ is unique to hematophagous organisms like malaria parasites and has been a preferential target for antimalarial drug design. Pathological studies of the malaria's intra-erythrocytic cycle show that severe modifications occur in the infected red blood cells (iRBC), including (i) an order-of-magnitude increase in cell stiffness related with a clearly diminished deformability and (ii) formation of adhesive "knobs" at the iRBC surface (which are electron-dense nanoscale protrusions on the surface of *P. falciparum*-iRBC) that allow cytoadherence to endothelial cells at the internal walls of blood vessels. Cytoadherence prevents mature iRBCs from reaching the spleen, where they would be cleared from the bloodstream due to their reduced deformability [3-6, 8-11]. However, the resulting microvascular obstruction leads to vital organ dysfunction, particularly in the brain and placenta, leading respectively to cerebral and placental malaria, which are often fatal.

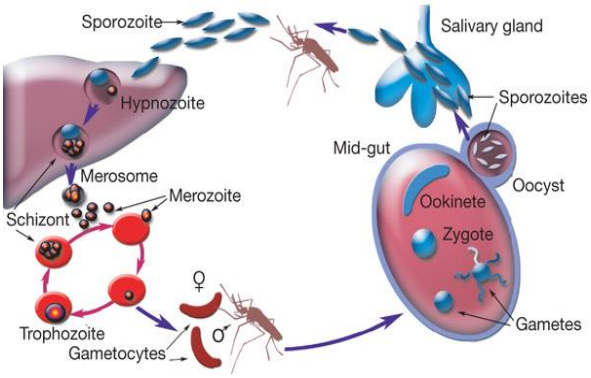

Figure 2 – Life cycle of malaria [13].

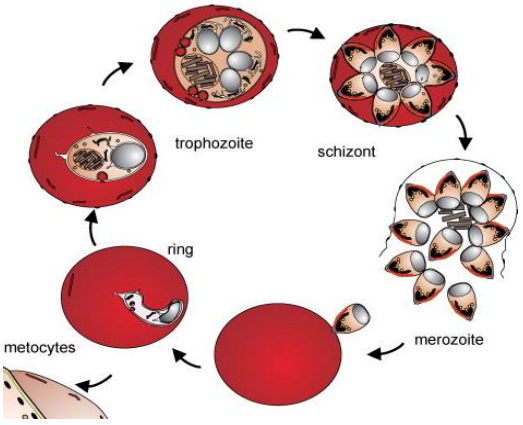

Figure 3 – The intra-erythrocytic cycle [16].

1. Objectives

1.1. Geral objetives

In viable parasites the hemozoin crystals move in the parasite vacuole [9-11] and this dynamic process of crystal growth, which to the best of my knowledge has not been investigated, may represent the means for an efficient collection of crystallizing units and the phenomenon calls for renovated attention. The apparently high driving force involved in this activity suggests that the phenomenon plays a vital role and that forced immobilization may lead to parasite destruction. The movement of hemozoin crystals and its possible damping by physical/chemical means, needs to be addressed from an engineering perspective and elucidating the details of the dynamic behavior of hemozoin crystals constitutes the purpose of the present work. The study of HZ movement may provide an innovative approach for parasite elimination and this preliminary investigation may raise interest on the potential of transforming HZ movement into a target for innovative therapies.

1.2. Specific objective

The movement of hemozoin crystals in the digestive vacuole of parasites in late trophozoite stage was studied by real-time microscopy (RTM) using a video camera coupled to an optical microscope. Parasites of the 3D7 and 2D2 strains were used in the investigations. The study aims to characterize the dynamic behavior of hemozoin crystals cultured at healthy body temperature and after exposure to febrile temperatures. The higher temperature is expected to stall the crystal movement and the possible resuming of movement will also be evaluated.

3. Materials and methods

3.1. Cultures

The *Plasmodium falciparum* species was selected for the investigation, as it is the deadliest of the malaria parasites and the only that can be maintained in culture. As mentioned above, there are dozens of strains of *P. falciparum* resistant and susceptible to different types of drugs. The strains investigated were the well-known 3D7 (susceptible to chloroquine and mefloquine) and DD2 (resistant to chloroquine and mefloquine). The 3D7 is the "type strain" of *P. falciparum* used as a basis to total genome sequencing which is deposited on PlasmoDB (http://plasmodb.org/plasmo/). Only late stage trophozoites were studied to better observe the hemozoin changes.

The parasite cultivation followed the following protocol: *P. falciparum* 3D7 and DD2 strains were continuously cultured and synchronized as previously described by Trager and Jensen (1976) [25], with minor modifications. Briefly, parasites were cultivated on human erythrocytes suspended in RPMI 1640 medium supplemented with HEPES, hypoxanthine and 10% AlbuMAX II, at pH 7.2. Cultures were maintained at 37ºC under an atmosphere of 5% CO_2 and synchronized by sorbitol treatment (Lambros and Vanderberg, 1979) [26] prior to the experiments. Stages and parasitaemia were determined by light microscopy observation of Giemsa-stained thin blood smears. These cultures were cultured at Instituto de Higiene e Medicina Tropical (IHMT) and the infected red blood cells were brought to IST under controlled temperature conditions for the measurements.

3.2. Microscope

An inverted IX51 microscope from Olympus was used with an oil immersion objective of 100x magnification with a numerical aperture 1.3 and working distance of 0.2 mm. The immersion oil used had a refraction index of 1.3. A drop was placed on the slide and the lens was lifted until it touched the droplet. The oil acted hence as a bridge between the glass plate and the glass lens focusing light rays and preventing dispersion. The larger cone of light entering the lens contributes to increasing the resolution and definition of the image.

The quality of an image depends on the resolution and ability of the lens to enlarge the specimen. The resolving power is the ability of the microscope to distinguish between two adjacent points as given by Rayleigh criterion (see equation 1).

$$\rho = \frac{1.22\,\lambda}{NA_{obj}+NA_{cond}} \qquad \text{(Equation 1)}$$

Where ρ is the resolved distance limit, λ is the wavelength of light, NA is the numerical aperture given by $n \times \sin\mu$ - where n is the refractive index of the medium between the object and the lens and where μ is the half-opening angle formed by the optical axis and the external rays of the beam of light penetrating the lens, *obj* is the objective and *cond* is the condenser.

The maximum resolution limit of the optical system employed is approximately 300 nm (for a condenser numerical aperture of 0.95 and considering an average wavelength of 550 nm). As the hemozoin crystals are typically 800x200x200 nm [29], the system cannot resolve the crystals width but can resolve their length. Higher resolution techniques, such as scanning or transmission electron microscopy (SEM and TEM, respectively) require vacuum and are not compatible with living parasites. Figures 5 and 6 show the size and morphology of post-mortem hemozoin crystals.

The Rayleigh criterion refers to a x,y plane perpendicular to the optical axis, while the resolution at along this axis (z), designated by depth of field, is given by [24]:

$$d = \frac{\lambda\sqrt{n^2-(NA)^2}}{(NA)^2} \qquad \text{(Equation 2)}$$

Where λ is the wavelength of light, n is the refractive index of the medium between the object and the lens and NA is the numerical aperture of the objective.

The depth of field of the present system is 253 nm. As the hemozoin crystals are in constant motion their (projected) x,y path can only be tracked within the depth of field.

3.3. Camera

Two high-speed cameras were used in the present work:

- Mega Speed MS70K camera from Canadian Photonics Laboratories with a maximum resolution of 512x512 capable of recording 1 fps to 100,000 fps; [19]
- FastCam SA3 model 120k from Photron with a 1024x1024 pixel resolution at frame rates up to 2,000 fps and at reduced resolution up to 120,000 fps. [20]

The images acquired with the Mega Speed MS70K camera resulted in lower spatial resolution and, for this reason most of the experiments were carried out using the FastCam camera (see Figure 4).

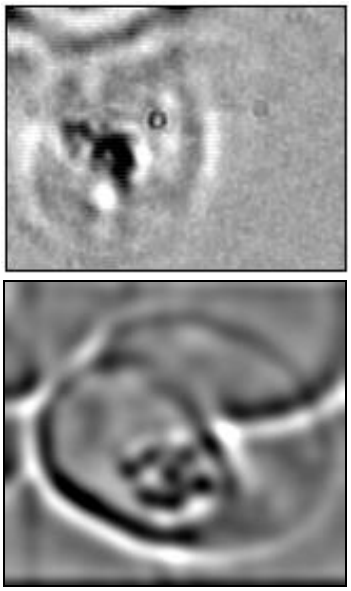

Figure 4 – Frame acquired with MegaSpeed (above) and frame acquired with FastCam (below).

4. Setup for image acquisition

The camera was coupled to the microscope setup. The sample was prepared by depositing 50 μl of a diluted cell suspension on a slide previously treated with poly-lysine (this substance provides grip and prevents cell drift

under observation). A coverslip was then placed on top of the cell suspension and the set was placed on the microscope stage after depositing a drop of immersion oil on the objective lens. The condenser diaphragm was opened to maximize resolution and after selecting a cell with clearly visible hemozoin crystals the images were acquired at 2128 fps using the Mega Speed camera and at 4000, 7500 and 15000 fps with the FastCam camera. Acquisitions at higher frame rates could not be carried out due to the drastic reduction in intensity and field of view. The movement was characterized at 20ºC for cells kept at healthy body temperature (37ºC) up to the experiment and for cells exposed to febrile temperature (40 ºC or 41 ºC for 1h) immediately prior to the experiments. The measurements were obtained from 10 cells: 7 trophozoites of the 3D7 strain and 3 trophozoites of the Dd2 strain.

4.1. Data processing (ImageJ and MATLAB)

Band pass filtering and segmentation of the images, as well as the determination of the (x,y) projected centroid for each particle, were carried out with a routine developed for ImageJ. The frame sequences were analyzed with routines developed for MATLAB to obtain:

A. Determination of the maximum displacement between any pair of points of a particle path (see Figure 9 (c)). Figure 68 shows the results from this analysis and the corresponding average velocity is summarized in Table 5.
B. Determination of the maximum displacement between any pair of points in sets of paths assumed to correspond to the same particle (as indicated in Figures 69 to 73). The average velocity resulting from this analysis is summarized in Table 6.

5. Results and discussion

Although the velocity values in tables 5 and 6 are varying with the acquisition rate, the fact that for 4000 and 7500 fps they do not scale with the frame rate suggests that the influence of noise is lower than is the previous analyses. However, the high standard deviation values indicate a low precision and these results may not reflect the true characteristics of the hemozoin crystals' movement.

Variable / frame rate	4000 fps Pixel: 10 nm	7500 fps Pixel: 10 nm	15000 fps Pixel: 10 nm
Displacement (µm)	0.074 ± 0.009	0.080 ± 0.011	0.072 ± 0.008
#frames	10.92 ± 9.93	12.76 ± 5.83	16.89 ± 6.26
Velocity (µm/s)	34.06 ± 13.61	49.05 ± 16.26	143.42 ± 149.27

Table 5 – Average velocity and average displacement of a particle with respective standard deviations determined from the maximum displacements of each individual path.

Variable / frame rate	4000 fps Pixel: 10 nm	7500 fps Pixel: 10 nm	15000 fps Pixel: 10 nm
Displacement (µm)	0.200 ± 0.041	0.211 ± 0.066	0.237 ± 0.077
#frames	130.20 ± 99.75	194.00± 135.78	222.33 ± 260.83
Velocity (µm/s)	10.96 ± 9.30	14.49 ± 15.15	29.96 ± 24.34

Table 6 – Average velocity and average displacement of a particle with respective standard deviations determined from the maximum displacements in sets assumed to correspond to the same particle (indicated in Figures 69 to 73).

Although the velocity values in tables 5 and 6 are varying with the acquisition rate, the fact that for 4000 and 7500 fps they do not scale with the frame rate suggests that the influence of noise is lower than is the previous analyses. However, the high standard deviation values indicate a low precision and these results may not reflect the true characteristics of the hemozoin crystals' movement.

5.1.1. Re-analysis of frames acquired with the Mega Speed MS70K Camera.

Since the values of velocity retrieved from the centroid positions in sequences acquired at 4000, 7500 and 15000 fps have low

precision, spots have also been visually tracked in the images acquired at 2128 fps with the Mega Speed MS70K Camera. For comparison, this analysis has also been performed for sequences acquired at 4000 fps with the FastCam Camera. The approach could not be carried out for the sequences acquired at 7500 or 15000 fps due to intense flickering and reduced acquisition times which made difficult tracking individual spots.

In total, 51 spots in the digestive vacuole of 3 different parasites have been tracked at 2128 fps and 21 spots in the digestive vacuole of 3 different parasites have been tracked at 4000 fps, both for the 3D7 strain. The results from this analysis are summarized in Table 7.

Variable/frame rate	2128 fps pixel: 50 nm	4000 fps pixel: 50 nm
Displacement (µm)	0.236 ± 0.090	0.190 ± 0.083
#frames	10.9 ± 2.5	12.6 ± 4.0
Velocity (µm/s)	52.5 ± 21.3	64.7 ± 25.2

Table 7 – Average values with respective standard deviations.

The fact that the velocity is not scaling with the frame rate and the lower standard deviations indicate that this analysis is more robust than the previous ones. The projected velocity of the hemozoin particles is close to 60 µm/s.

5.1.2. Temperature effect

In general, after exposure to febrile temperatures (40 °C or 41 °C for 1h) the movement of the crystals ceased. The loss of movement of hemozoin crystals can be considered one of the first indicators of an adverse response of the parasite to external stimuli, before distinct morphological changes occur [10]. After the heat treatment at 41 °C virtually all parasites exhibited immobile hemozoin crystals, while after the heat treatment at 40 °C some parasites still presented moving crystals. Therefore, contrarily to what has been stated in the literature [10], the motion of hemozoin is not Brownian in nature since the velocity does not increase with temperature and the crystals do not move in dead parasites. The fact that for the parasites exposed at 40 °C some particles resumed motion after 1 hour at room temperature is noteworthy. A quantitative characterization of the effect of febrile temperatures requires the development of an experimental protocol for image acquisition suitable to analyze the motion of the hemozoin crystals with higher accuracy and precision.

6. Conclusions

The results obtained from real-time microscopy and their analysis enable to infer that:

- The projected movement, although irregular, is compatible with a reciprocating nature and may be associated with rotation;
- The average (projected) translation velocity measured at 2128 fps is 52.5 ± 21.3 µm/s while the value obtained from measurements at 4000 fps is 64.7 ± 25.2 µm/s.
- The average free path of each particle was 0.236 ± 0.090 µm for the measurements carried out at 2128 fps and 0.190 ± 0.083 for the measurements carried out at 4000 fps.
- The crystal rotation halts after exposure to 41 °C for 1 h. After exposure at 40 °C for 1 h most crystal movement stops, however, partial resuming has been observed after 1 h at room temperature.
- The crystal movement observed has not a Brownian nature as it does not increase with temperature and the crystals do not move in dead parasites.

The dynamic behavior observed is expected to be associated with a relatively high driving force and to involve significant energy consumption. One hypothesis that remains to

be proven is that it represents the means for an efficient collection of the crystallizing units.

7. Future work

As future work I suggest the acquisition of frames at rates between 2000 and 4000 fps using a camera with high resolution in order to visualize the particles' movement and follow their path with lower noise.

The fact that the particles' movement is dampen with exposure to fever and can partially resumed after fever exposure shows that the effect of temperature is not well understood and that the phenomenon demands a deeper investigation. In addition to the effect of drugs, the effect of electrical and magnetic fields on the movement of the paramagnetic hemozoin crystals is also worth studying.

A precise characterization of the hemozoin crystals' movement is necessary to cast new light on the driving forces behind this dynamic behavior and this approach is expected to pave the way for novel therapies and diagnostic tools.

8. References

[1] Newton C, Krishna S, Severe Falciparum Malaria in Children: Current Understanding of Pathophysiology and Supportive Treatment, Pharmacology & Therapeutics, Volume 79, Issue 1, July 1998, Pages 1–53;

[2] Crawley J, Nahlen B, Prevention and treatment of malaria in young African children, Seminars in Pediatric Infectious Diseases, Volume 15, Issue 3, July 2004, Pages 169–180;

[3] Santos-Magalhães N S, Mosqueira V C F, Nanotechnology applied to the treatment of malaria, Advanced Drug Delivery Reviews, Volume 62, Issues 4–5, 18 March 2010, Pages 560–575;

[4] Jerrard D A, Broder J S, Hanna J R, Colletti J E, Grundmann K A, Geroff A J, Mattu A, Malaria: a rising incidence in the United States, The Journal of Emergency Medicine, Volume 23, Issue 1, July 2002, Pages 23–33;

[5] Wykes M N, Horne-Debets J, Dendritic cells: The Trojan horse of malaria?, International Journal for Parasitology, Volume 42, Issue 6, 15 May 2012, Pages 583–587;

[6] Goldberg DE, A F Slater, A Cerami, G B Henderson. Hemoglobin degradation in the malaria parasite Plasmodium falciparum: an ordered process in a unique organelle. Proc Natl Acad Sci U S A. 1990 April; 87(8): 2931–2935;

[7] Butykai, A. et al. Malaria pigment crystals as magnetic micro-rotors: key for high-sensitivity diagnosis. Sci. Rep. 3, 1431; DOI:10.1038/srep01431 (2013);

[8] Biagini GA, Bray PG, Spiller DG, White MR, Ward SA. The digestive food vacuole of the malaria parasite is a dynamic intracellular Ca2+ store. J Biol Chem. 2003 Jul 25;278(30):27910-5. Epub 2003 May 8. PubMed PMID: 12740366;

[9] Carvalho PA, Diez-Silva M, Chen H, Dao M, Suresh S. Cytoadherence of erythrocytes invaded by Plasmodium falciparum: quantitative contact-probing of a human malaria receptor. Acta Biomater. 2013 May;9(5):6349-59.

[10] Sachanonta N, Chotivanich K, Chaisri U, Turner GD, Ferguson DJ, Day NP, Pongponratn E. Ultrastructural and real-time microscopic changes in P. falciparum-infected red blood cells following treatment with antimalarial drugs. Ultrastruct Pathol. 2011 Oct;35(5):214-25;

[11] Effects of antimalarial drugs on movement of Plasmodium falciparum, http://www.ncbi.nlm.nih.gov/pubmed/23082547

[12] http://www.who.int/mediacentre/factsheets/fs094/en/

[13] Winzeler EA, Malaria research in the post-genomic era, Nature 455 (2008) 751-756

[14] John E. Hyde, Drug-resistant malaria - an insight, FEBS Journal 274 (2007)

[15] The Lancet Infectious Diseases, Volume 13, Issue 2, Pages 114 - 115, February 2013

[16] Tilley et at. The Plasmodium falciparum-infected red blood cell, Int. J. Biochem Cell Biology 43 (2011) 839

[17] http://www.jn.pt/PaginaInicial/Sociedade/Interior.aspx?content_id=2066672

[18] http://www.publico.pt/ciencia/noticia/portugueses-estao-a-desenvolver-uma-vacina-contra-a-malaria-1613253#/0

[19] http://www.cplab.com/index.htm

[20] http://www.photron.com/?cmd=product_general&product_id=6

[21] http://www.thelancet.com/journals/laninf/article/PIIS1473-3099%2812%2970349-3/fulltext

[22] Rosario V. Cloning of naturally occurring mixed infections of malaria parasites. Science. 1981 May 29;212(4498):1037-8. PubMed PMID: 7015505.

[23] http://micro.magnet.fsu.edu/primer/anatomy/immersion.html

[24] http://micro.magnet.fsu.edu/primer/anatomy/focusdepth.html

[25] Trager W, Jensen JB. Human malaria parasites in continuous culture. Science. 1976 Aug 20;193(4254):673-5.

[26] Lambros C, Vanderberg JP. Synchronization of Plasmodium falciparum erythrocytic stages in culture. J Parasitol. 1979 Jun;65(3):418-20.

[27] Esposito A, Tiffert T, Mauritz JMA, Schlachter S, Bannister LH, et al. (2008) FRET Imaging of Hemoglobin Concentration in *Plasmodium falciparum*-Infected Red Cells. PLoS ONE 3(11): e3780. doi:10.1371/journal.pone.0003780

[28] Johann, L., Lanfranchi, D. A., Davioud-Charvet, E., & Elhabiri, M. (2012). A Physico-Biochemical Study on Potential Redox-Cyclers as Antimalarial and Antischistosomal Drugs. *Current Pharmaceutical Design*, *18*(24), 3539–3566.

[29] Carvalho P.A., L. Coelho, R.C. Martins and F. Nogueira. Differences between synthetic ß-haematin and native hemozoin crystals. Microscopy and Microanalysis. 2013 19 (Suppl. 4), pp 49-50. doi:10.1017/S143192761300086X. IF 2.992

[30] http://www.vtnews.vt.edu/articles/2008/05/2008-322.html

[31] Goldberg, Daniel E; .Complex nature of malaria parasite hemoglobin degradation, vol. 110 no. 14, 5283-5284, 2013;

[32] Kapishnikov, Sergey et al; Oriented nucleation of hemozoin at the digestive vacuole membrane in *Plasmodium falciparum*, vol. 109 no. 28, 11188-11193, 2012